MIPAS Ultimate Retrieval Accuracy
Final Report
PO-TN-OXF-GS-0014
Task 4.3, CCN5 11886/96/NL/GS

Anu Dudhia *

19th June, 2000

Abstract

This report assesses the ultimate retrieval accuracy that could be obtained by MIPAS if there were no limit on the number of measurements used in the retrieval. The analysis is performed for each of the 7 target species (pT, CH_4, H_2O, HNO_3, N_2O, NO_2 and O_3), assuming a measurement sequence of 16 spectra from 8–53 km in 3 km steps, with profiles retrieved at the tangent points.

The accuracy is defined in terms of the 'total retrieval error', which includes estimates of all known systematic error sources as well as the random component due to instrument noise (with the caveat that uncertainties in the *absolute* values of HITRAN line strengths have not been considered).

The measurements are selected using the Oxford microwindow program which is run until no more microwindows can be found that improve the the retrieval.

The sensitivity of the results to the selection criteria is discussed in an Appendix.

Apart from the results, the main conclusion is that the limiting accuracy in VMR retrievals is either instrument noise or, more usually, the assumed 3 K temperature uncertainty, a somewhat arbitrary figure which perhaps should be re-assessed. Also, that while several hundreds of microwindows can be found, there are no obvious optimum points at which to truncate the microwindow list.

1 Introduction

Operational constraints require that processing of MIPAS data in real time is restricted to using a few tens of microwindows per species, and various objective schemes[1][2][3] have been developed in order to select the optimum microwindows.

This study assesses the accuracy that could be obtained if there were no such constraints. The procedure is to use the Oxford microwindow selection program `MWMAKE`[2][3], and simply continue to select microwindows until the accuracy can be improved no further.

A useful feature of the microwindow selection process is that not only does it simulate the retrieval error due to random noise, it also quantifies the effect of the various sources of systematic error, allowing a 'total error' for the retrieval to be defined and analysed.

2 Error sources

The 'random error' is defined as the error due to noise, based on the instrument test results supplied by ESA[4]. This is then apodised, which has the effect of reducing the amplitude and creating correlations between adjacent spectral points.

The 'systematic error' covers all other known error sources, which are correlated over larger scales. Except where otherwise stated, the individual systematic errors are assumed to be correlated for all measurements. The errors considered are:

Contaminant uncertainties Each species is assumed to be known to a limited accuracy, taken as 1/6th of the difference (in log-space) of minimum and maximum profiles for each species[5]. The min and max are assumed to represent $\pm 3\sigma$ variations about a mean, hence 1σ uncertainty is estimated by taking 1/6 of this variability. No assumptions are made about the sequence of retrievals (other than that the pT retrieval is first), hence 'climatological' uncertainties are assumed for all contaminants. These error contributions

*Atmospheric, Oceanic and Planetary Physics, Oxford University, UK

are listed in Tables 1–7 by their chemical formulae.

Gain Errors Assumed to be 2% uncertainty. Uncorrelated between microwindows. Listed as '`gain`' in the tables.

Hitran Errors Based on a perturbing line parameters by a typical uncertainty, as used in the microwindow study[6]. Uncorrelated between different microwindows. This does not allow for the uncertainties in *absolute* line strength, only relative uncertainties between bands (line strength errors map directly into errors in retrieved concentrations). Listed as '`hitran`' in the tables.

Temperature Errors Assumed to be 3 K. This figure partly arises from the assumed pT retrieval error (1 K), but mostly represents an uncertainty due to horizontal temperature gradients in the line-of-sight. Applied to constituent retrievals only. Uncorrelated between altitudes. Listed as '`tem`' in the tables.

Pointing Errors Assumed to be 150 m (=2% in tangent pressure). Also arising from the pT retrieval. (NB: This only represents the error in retrieving tangent point VMR given an incorrect tangent point pressure, and does not include the often larger error associated with steep VMR gradients as a function of pressure.) Applied to constituent retrievals only. Uncorrelated between altitudes. Listed as '`los`' in the tables.

Non-LTE Errors Effect of neglecting non-LTE effects, using calculations performed for microwindow study[6]. Listed as '`nonlte`' in the tables.

Spectral Calibration Errors Assumed to be 0.001 cm^{-1}, expected residual error from the MIPAS in-flight spectral calibration. Listed as '`shift`' in the tables.

Continuum Parametrisation Errors The magnitudes of the various gaseous continuum absorption coefficients (H_2O, CO_2, N_2, O_2) are assumed to have an uncertainty of 25%. Listed as '`ctmerr`' in the tables.

3 Microwindow Selection

The Oxford multilayer microwindow selection program `MWMAKE` is used to construct/select microwindows sequentially. Having determined a suitable single measurement (specified on the 0.025 cm^{-1} wavenumber grid and 3 km tangent altitude grid) as a 'starting point', microwindows are 'grown' by gradually including adjacent points until either no further points are found which improve the retrieval, or (occasionally) the imposed limit of 3 cm^{-1} width is reached. This gives a maximum of 1936 measurements in a microwindow (=121 spectral points × 16 altitudes). While the microwindow is nominally 'rectangular', being defined by pairs of wavenumber and altitude boundaries, this procedure also generates 'spectral masks': internal points can be excluded from the microwindow if they increase the total error (this may arise because measurement contributions to the retrieval are weighted only by the random error and not the total error).

Since there is no guarantee that the best starting point will grow into the best microwindow, new microwindows are actually grown from 99 different starting points, compared, and only the best is used. The retrieval errors are then modified to include this microwindow, a new set of trial starting points selected and the process repeated.

For the VMR retrievals, the retrieval state vector contains 16 elements corresponding to the VMR at the tangent altitudes, plus one element for every microwindow corresponding to the offset retrieval, and one element for every microwindow altitude at or below 29 km for the continuum retrieval (i.e., offset and continuum profiles are retrieved independently for each microwindow).

The use of instrument pointing information in the operational pT retrieval is simulated by retrieving a single reference pressure along with 16 tangent temperatures. Effectively, this is assuming perfect relative pointing knowledge but poor absolute pointing.

To begin the selection, the program requires an *a priori* estimate of retrieval uncertainty (random error), and this is set to 100% for constituent VMR, 10 K for temperature, 10% for reference pressure, 1000% for continuum and the NESR for the offset.

Where the final retrieval uncertainty falls to less than 10% VMR or 1 K temperature, it can be assumed that the result would be the same as that obtained using a least-squares fit without any influence from the *a priori*.

4 Defining 'Accuracy'

The program evaluates improvement in retrieval accuracy in terms of the increase in a 'figure of merit' H, which is itself is defined in terms of a decreasing 'error function' F

$$H = -\frac{1}{2}\log_2\left(F^{\mathrm{rtv}}/F^{\mathrm{apr}}\right) \qquad (1)$$

F is generally some scalar function of the random ($\mathbf{S}^{\mathrm{rnd}}$), systematic ($\mathbf{S}^{\mathrm{sys}}$) and/or requirement covari-

ance ($\mathbf{S}^{\mathrm{req}}$) for the retrieval. Since H increases monotonically as F decreases, the form of Eq. (1) serves only to define $H = 0$ as the merit associated with the *a priori* information alone, and a unit increment in H with a factor 4 reduction in F. It is the function F itself which determines the selection.

A simple form of F, here labelled F_0, considers only the total error,

$$F_0 = \prod_i S_{ii}^{\mathrm{tot}} = \prod_i \left(S_{ii}^{\mathrm{rnd}} + S_{ii}^{\mathrm{sys}}\right) \qquad (2)$$

where S_{ii} represent the diagonal elements of the covariance matrix, considering only elements $i = 1 \ldots 16$ corresponding to the profile of the target quantity, and excluding offset or continuum information. In this case a unit increment of H (1 'bit' of information) corresponds to a factor 2 reduction in the 1-σ uncertainty at one profile level. On all the plots in this report, retrievals have been *evaluated* using this function F_0 in order to provide a more meaningful number (in fact, a plot of the F_3 figure of merit generally follows a very similar curve, but with a vertical offset — see Appendix).

For the microwindow *selection* a slightly more complicated function, F_3, has been used:

$$F_3 = \prod_i \left(\frac{1}{4}S_{ii}^{\mathrm{rnd}} + \frac{3}{4}S_{ii}^{\mathrm{sys}} + S_{ii}^{\mathrm{req}}\right) \qquad (3)$$

This biases the selection towards microwindows with a relatively low systematic error compared to the random error, on the assumption that, while the random errors would continue to decrease as more microwindows are added, the systematic errors would ultimately be irreducible. Thus a lower final error should be obtainable if the systematic errors are kept low to start with (whether or not this is the case is examined in the Appendix). Having found all microwindows to maximise the F_3 function, the microwindow list was re-evaluated using the F_0 function and any further microwindows which improved F_0 then added.

The presence of the requirement covariance (25% VMR, 3 K) serves to bias the initial selection to improvement at altitude where the requirement is not met, but after that should have little further effect.

Also plotted on the 'Figure of Merit' graphs (using the right hand axis) are three curves illustrating the contributions of random and systematic errors to the total as more measurements are added. These are derived from the trace of the various error covariances

$$\sum_i \frac{S_{ii}^{\mathrm{rnd}}}{S_{ii}^{\mathrm{apr}}}, \qquad \sum_i \frac{S_{ii}^{\mathrm{sys}}}{S_{ii}^{\mathrm{apr}}}, \qquad \sum_i \frac{S_{ii}^{\mathrm{tot}}}{S_{ii}^{\mathrm{apr}}} \qquad (4)$$

Thus the total error starts at a figure of 1 before the first microwindow is selected, representing the *a priori* random component alone (since there is no *a priori* systematic error).

5 Results & Discussion

Results for each of the 7 retrievals are shown in Figs. 1–7 and Tables 1–7.

pT Retrieval accuracies 0.2–0.4 K at all altitudes. Gain, HITRAN and O_3 uncertainties are the major systematic error sources, and comparable to the random error. Surprisingly, non-LTE is also significant at lower altitudes. Microwindows are selected in all bands except C (the selection program requires some sensitivity to CO_2 for all *pT* microwindows, and there are no CO_2 lines in the C band), initially from the A band then, as these reduce in size, larger microwindows mostly from the D band. The switch from F_3 to F_0 at MW#3189 is evident in the sharp discontinuity in the Figure of Merit Curve (the last few microwindows selected with F_3 had actually been causing the F_0 Figure of Merit to reduce). Note that horizontal temperature gradients are only included in the 3 K temperature uncertainty used as input to the VMR selection, and are not considered in the *pT* selection itself.

CH_4 Above 29 km, retrieval accuracy is 10–15%, limited by temperature uncertainty. Below 29 km, retrieval accuracy is around 5%, limited by random errors. Below 20 km, the HITRAN uncertainty is the dominant systematic error source, although only contributing around 2% VMR error. Microwindows are small compared to other species, and concentrated in the B band, with some in the AB and C bands. The switch from F_3 to F_0 occurred at MW#839, but did not appear to lead to any significant change in behaviour.

H_2O Up to 20 km, retrieval accuracy is 4–7%, around 12% from 32 km upwards and around 10% from 23–29 km. The increase above 23 km is mainly due to the increased temperature systematic error which becomes dominant at higher altitudes. HITRAN uncertainties are the largest systematic error source from 14–20 km but in this altitude range the accuracy is limited by the random noise which remains around 2–5% for the whole profile from 11 km upwards. Behaviour at 8 km is very different: random noise is small (0.7%) but the non-LTE error of 3% is the largest error source. Microwindows are selected across the whole spectral range up to 2100 cm^{-1}, but there is a significant reduction in average size after the first 500 microwindows. The F_3/F_0 switch occurred at MW#2194, the last microwindows selected under F_3 evident as

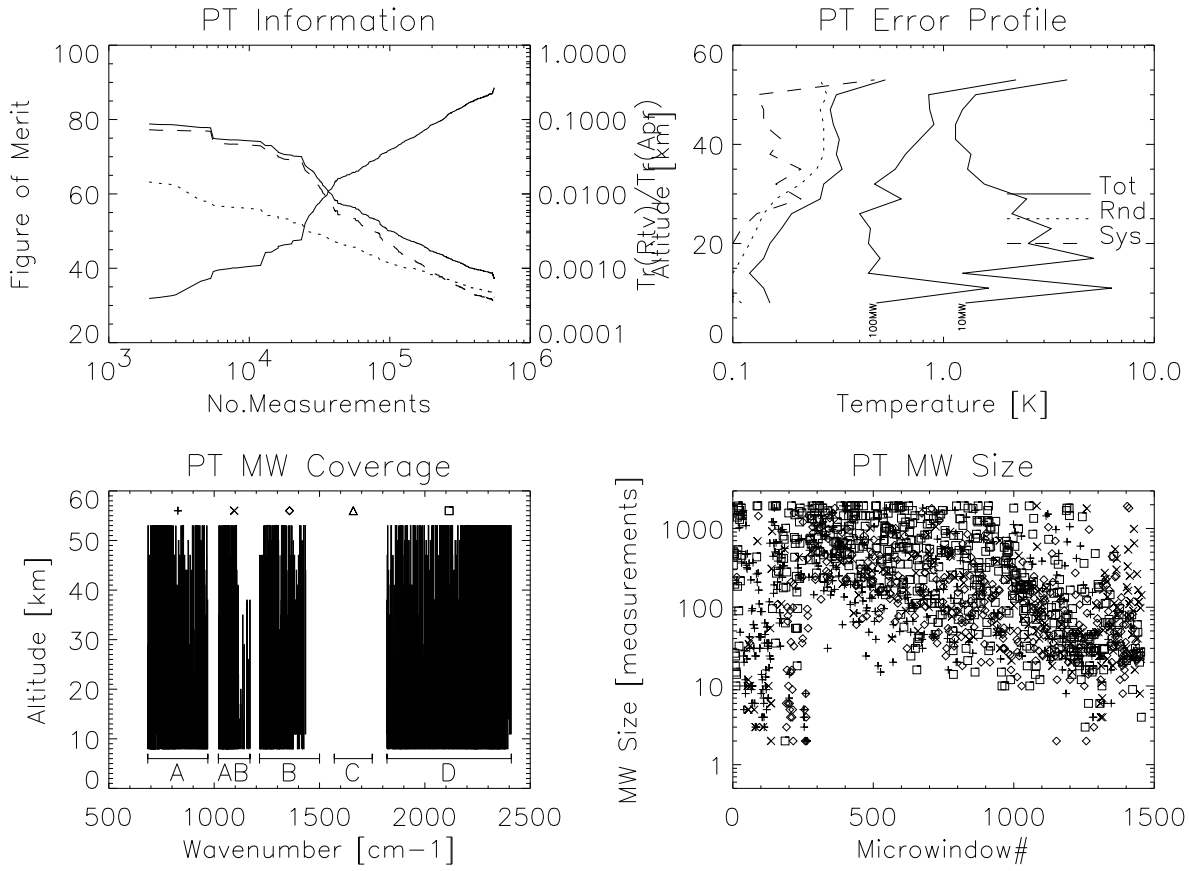

Figure 1: *pT* Results. Top left panel shows increase in information with number of measurements, along with reduction in trace of the error covariances (key as in top right). Top right shows final total error profile, together with profiles of the random and systematic error components. Also shown are the total error profiles after 10 and 100 microwindows have been selected. Bottom left plot shows wavenumber and altitude coverage of the microwindows. Bottom right plot shows band and size of microwindows as a function of selection number (see bottom left plot for key).

Table 1: *pT* Error contributions.

Microwindows = 3616					Average size = 131 meas./MW				Used/Total meas. = 167523/474478 (35%)								
Alt	8km	11km	14km	17km	20km	23km	26km	29km	32km	35km	38km	41km	44km	47km	50km	53km	
Rnd	0.1	0.1	0.1	0.1	0.1	0.1	0.1	0.1	0.1	0.1	0.2	0.2	0.2	0.2	0.2	0.2	
Sys	0.3	0.4	0.2	0.2	0.2	0.2	0.2	0.2	0.2	0.2	0.2	0.1	0.1	0.2	0.1	0.3	
Tot	0.3	0.4	0.2	0.2	0.2	0.2	0.2	0.3	0.2	0.3	0.3	0.2	0.2	0.2	0.2	0.4	
Significant systematic error sources																	
h2o	0.0	0.0	0.0	0.1	0.1	0.0	0.0	0.0	0.0	0.0	0.0	0.0	0.0	0.0	0.0	0.1	
o3	0.0	0.1	0.1	0.1	0.0	0.0	0.0	0.1	0.1	0.1	0.1	0.1	0.0	0.0	0.0	0.1	
n2o	0.1	0.1	0.0	0.0	0.0	0.0	0.0	0.0	0.0	0.0	0.0	0.0	0.0	0.0	0.0	0.1	
ch4	0.1	0.1	0.0	0.0	0.0	0.0	0.0	0.0	0.0	0.1	0.1	0.0	0.0	0.0	0.0	0.0	
hno3	0.1	0.1	0.0	0.0	0.0	0.0	0.0	0.0	0.0	0.0	0.0	0.0	0.0	0.0	0.0	0.1	
ccl4	0.1	0.1	0.0	0.0	0.0	0.0	0.0	0.0	0.0	0.0	0.0	0.0	0.0	0.0	0.0	0.0	
cof2	0.1	0.0	0.0	0.0	0.0	0.0	0.0	0.0	0.0	0.0	0.0	0.0	0.0	0.0	0.0	0.0	
nonlte	0.1	0.2	0.1	0.1	0.1	0.1	0.0	0.0	0.0	0.0	0.0	0.0	0.0	0.0	0.0	0.0	
hitran	0.1	0.1	0.0	0.1	0.1	0.1	0.1	0.1	0.1	0.1	0.1	0.1	0.1	0.1	0.1	0.1	
gain	0.1	0.2	0.1	0.1	0.1	0.2	0.1	0.2	0.1	0.1	0.1	0.1	0.1	0.1	0.1	0.2	
ctmerr	0.1	0.0	0.0	0.0	0.0	0.0	0.0	0.0	0.0	0.0	0.0	0.0	0.0	0.1	0.0	0.1	

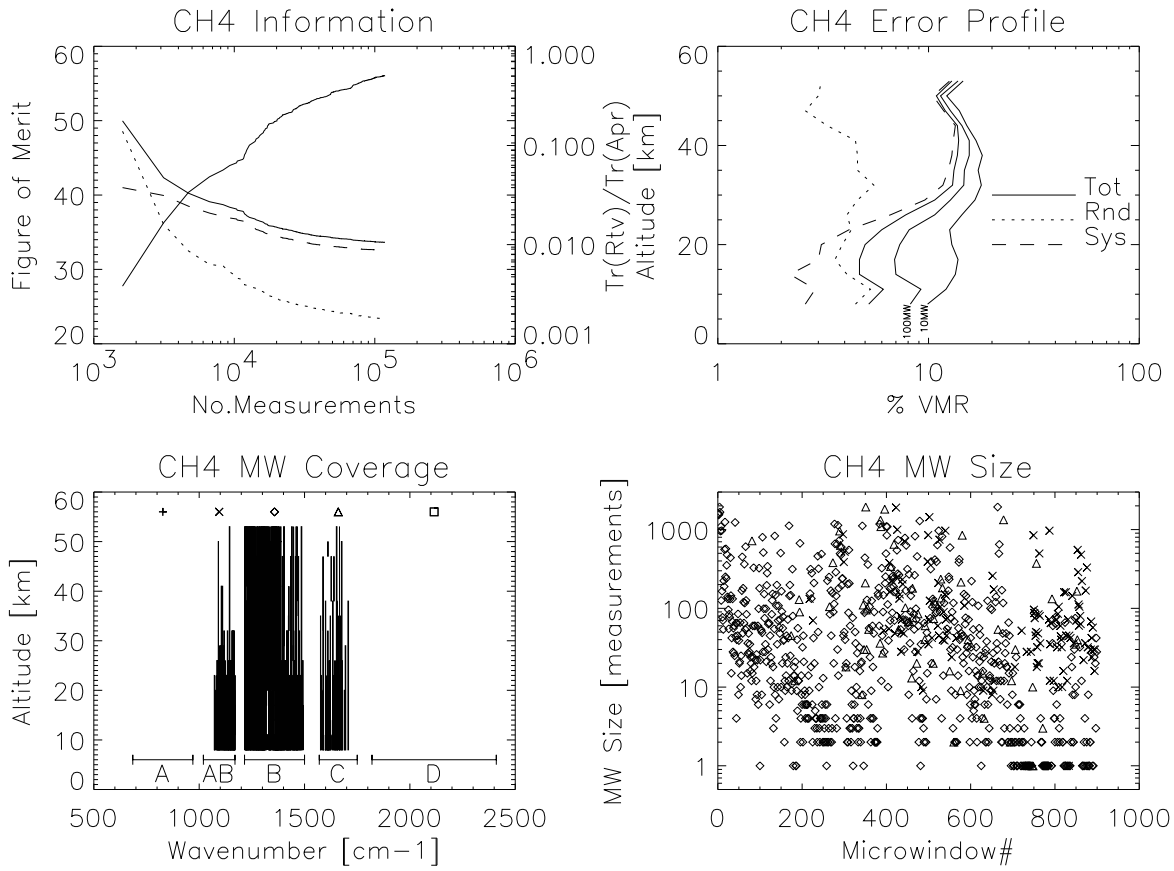

Figure 2: CH_4 Results. Top left panel shows increase in information with number of measurements, along with reduction in trace of the error covariances (key as in top right). Top right shows final total error profile, together with profiles of the random and systematic error components. Also shown are the total error profiles after 10 and 100 microwindows have been selected. Bottom left plot shows wavenumber and altitude coverage of the microwindows. Bottom right plot shows band and size of microwindows as a function of selection number (see bottom left plot for key).

Table 2: CH_4 Error contributions.

Microwindows = 899					Average size = 131 meas./MW					Used/Total meas. = 46157/117961 (39%)						
Alt	8km	11km	14km	17km	20km	23km	26km	29km	32km	35km	38km	41km	44km	47km	50km	53km
Rnd	4.6	5.3	4.1	3.6	3.9	4.3	4.1	4.6	5.5	4.6	4.6	4.5	3.3	2.6	3.0	3.1
Sys	2.6	2.9	2.2	3.0	3.1	4.2	6.6	9.6	11.7	12.4	12.9	13.1	13.4	11.8	10.5	12.6
Tot	5.2	6.1	4.7	4.7	5.0	6.0	7.8	10.7	13.0	13.2	13.7	13.9	13.7	12.0	10.9	12.9
Significant systematic error sources (largest error source at each altitude in bold):																
n2o	0.2	0.1	0.2	0.6	0.8	0.9	1.1	2.0	1.1	0.9	0.6	0.7	0.2	0.3	0.3	0.6
hno3	0.4	0.1	0.0	0.1	0.2	0.3	0.7	1.2	0.8	0.0	0.6	0.6	0.5	0.0	0.0	0.2
hocl	0.1	0.5	0.1	0.2	0.1	0.2	0.1	0.3	0.1	0.3	0.2	0.0	0.0	0.0	0.0	0.1
nonlte	0.0	0.0	0.0	0.0	0.0	0.3	0.3	0.7	0.0	0.4	1.6	1.5	1.9	1.1	0.6	8.0
hitran	**2.1**	**2.3**	**1.6**	**2.1**	**1.9**	2.3	2.4	3.3	2.7	2.6	1.9	1.1	1.4	0.8	0.6	1.0
gain	1.4	1.1	0.9	0.7	0.8	1.3	0.9	1.1	1.0	1.1	1.2	1.0	1.5	1.0	0.9	1.5
tem	0.5	1.0	0.8	1.7	**1.9**	**2.8**	**5.5**	**8.0**	**10.6**	**11.5**	**12.2**	**12.7**	**12.9**	**11.4**	**10.3**	**9.3**
los	0.5	0.7	0.5	0.7	0.9	1.2	1.9	2.8	3.2	3.2	2.8	2.1	2.0	2.0	2.0	2.0

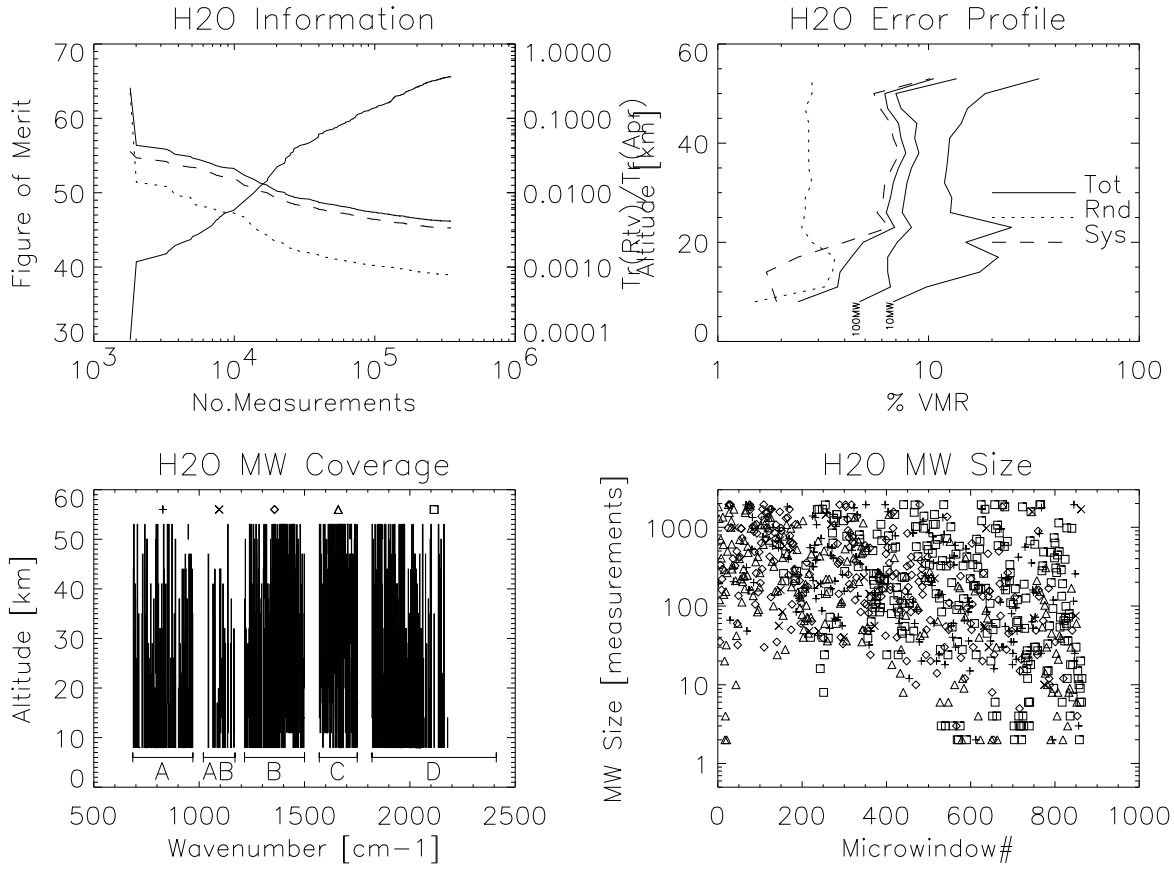

Figure 3: H_2O Results. Top left panel shows increase in information with number of measurements, along with reduction in trace of the error covariances (key as in top right). Top right shows final total error profile, together with profiles of the random and systematic error components. Also shown are the total error profiles after 10 and 100 microwindows have been selected. Bottom left plot shows wavenumber and altitude coverage of the microwindows. Bottom right plot shows band and size of microwindows as a function of selection number (see bottom left plot for key).

Table 3: H_2O Error contributions.

Microwindows = 2241					Average size = 151 meas./MW					Used/Total meas. = 131306/338286 (39%)						
Alt	8km	11km	14km	17km	20km	23km	26km	29km	32km	35km	38km	41km	44km	47km	50km	53km
Rnd	0.7	2.1	4.5	5.9	5.2	3.6	4.0	4.2	4.0	4.1	3.4	1.9	2.1	2.6	3.7	4.5
Sys	4.6	3.7	1.9	1.7	4.4	8.5	8.3	9.5	12.1	11.2	11.1	12.4	11.9	11.6	11.5	12.2
Tot	4.7	4.2	4.9	6.1	6.8	9.2	9.2	10.4	12.7	12.0	11.6	12.5	12.1	11.9	12.0	13.0
Significant systematic error sources (largest error source at each altitude in bold):																
o3	0.4	0.1	0.2	0.1	0.4	1.8	2.6	2.9	2.6	1.5	1.2	0.3	0.1	0.3	0.3	0.5
ch4	0.3	0.2	0.0	0.4	0.3	2.5	2.8	2.4	2.2	1.6	1.4	0.6	0.5	0.8	0.8	0.8
nonlte	**3.0**	0.6	0.2	0.0	0.1	0.2	0.1	0.1	0.7	0.8	0.7	1.9	2.0	2.2	4.0	5.2
hitran	1.1	1.5	**1.4**	**1.3**	**2.9**	2.1	2.8	3.1	2.8	3.1	2.5	3.3	2.8	3.8	2.5	1.8
gain	1.2	1.8	0.5	0.6	1.3	0.6	1.2	1.1	0.9	0.7	0.7	0.8	0.7	1.3	0.9	1.5
ctmerr	0.5	1.1	0.0	0.2	0.3	0.2	0.1	0.5	0.9	0.4	0.4	0.2	0.1	1.3	0.0	0.2
tem	2.7	**2.1**	0.8	0.5	2.7	**7.0**	**5.8**	**7.3**	**10.1**	**9.7**	**9.8**	**11.1**	**10.7**	**10.0**	**10.0**	**10.5**
los	1.2	1.0	0.7	0.5	1.1	1.8	1.8	2.4	3.6	3.7	3.7	3.9	3.8	3.3	2.7	2.3

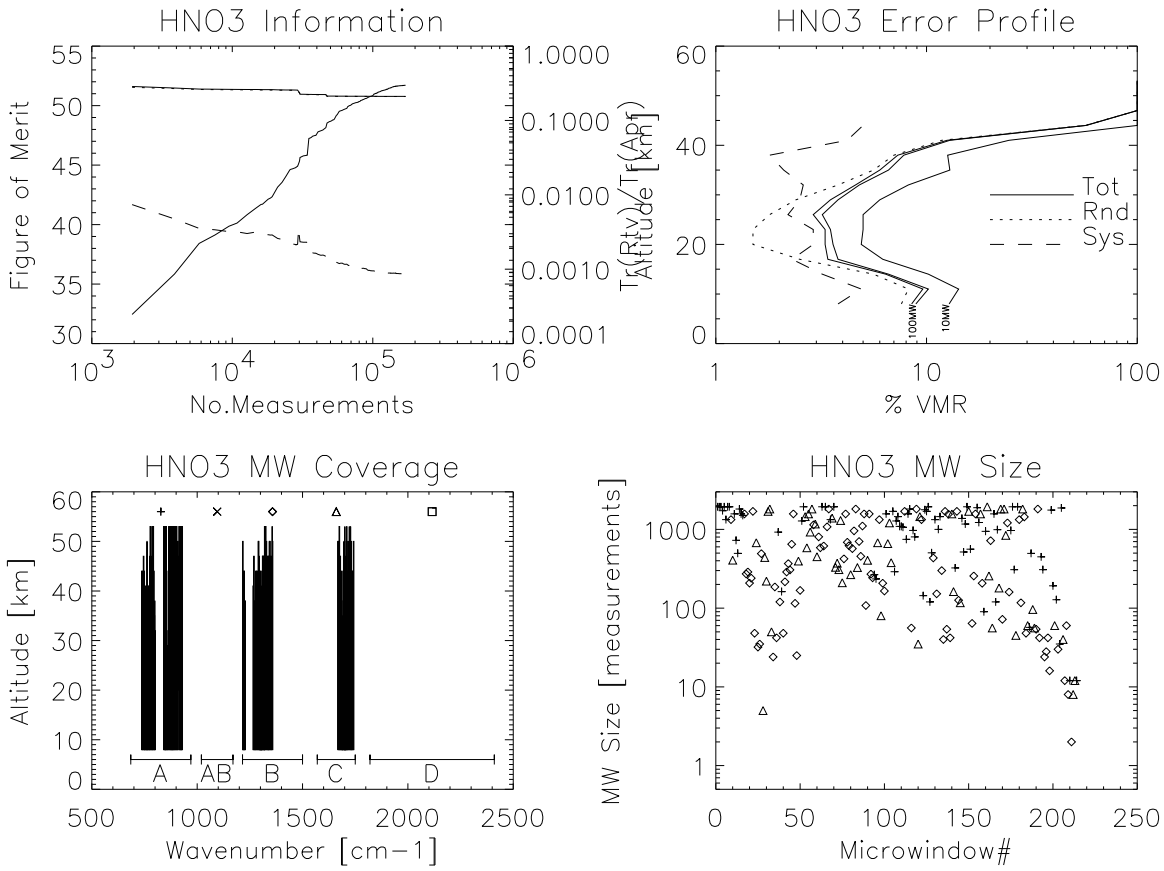

Figure 4: HNO_3 Results. Top left panel shows increase in information with number of measurements, along with reduction in trace of the error covariances (key as in top right). Top right shows final total error profile, together with profiles of the random and systematic error components. Also shown are the total error profiles after 10 and 100 microwindows have been selected. Bottom left plot shows wavenumber and altitude coverage of the microwindows. Bottom right plot shows band and size of microwindows as a function of selection number (see bottom left plot for key).

Table 4: HNO_3 Error contributions.

Microwindows = 449					Average size = 297 meas./MW					Used/Total meas. = 52427/133375 (39%)						
Alt	8km	11km	14km	17km	20km	23km	26km	29km	32km	35km	38km	41km	44km	47km	50km	53km
Rnd	8.1	8.7	6.3	2.9	1.8	1.7	2.3	2.8	3.3	5.7	8.8	16.1	63.6	100	100	100
Sys	4.8	5.3	5.1	5.7	6.9	6.1	4.5	4.4	6.2	5.1	3.2	4.0	4.8	0.0	0.0	0.0
Tot	9.4	10.2	8.1	6.4	7.1	6.3	5.1	5.2	7.0	7.7	9.4	16.6	63.7	100	100	100
Significant systematic error sources (largest error source at each altitude in bold):																
n2o	1.2	0.7	0.5	0.1	0.1	0.9	0.6	0.3	0.2	0.0	0.2	0.0	0.4	0.0	0.0	0.0
ch4	0.5	0.7	0.5	0.3	0.0	0.5	0.6	0.8	0.5	0.1	0.0	0.1	1.3	0.0	0.0	0.0
hitran	2.0	2.7	2.7	2.1	1.7	2.4	1.9	1.7	2.5	2.1	1.6	**3.0**	1.9	0.0	0.0	0.0
gain	**3.0**	2.3	1.7	1.3	1.3	1.2	1.2	1.0	1.1	1.0	0.7	1.8	1.5	0.0	0.0	0.0
shift	0.2	0.5	0.4	0.1	0.0	0.1	0.5	0.4	0.2	0.1	0.4	0.1	1.6	0.0	0.0	0.0
tem	2.6	**3.5**	**3.7**	**5.0**	**6.4**	**5.1**	**3.4**	**3.4**	**4.9**	**4.0**	**2.5**	1.8	**2.9**	0.0	0.0	0.0
los	0.5	0.9	1.0	1.1	1.3	1.3	1.1	1.2	1.9	1.7	0.9	0.6	0.4	0.0	0.0	0.0

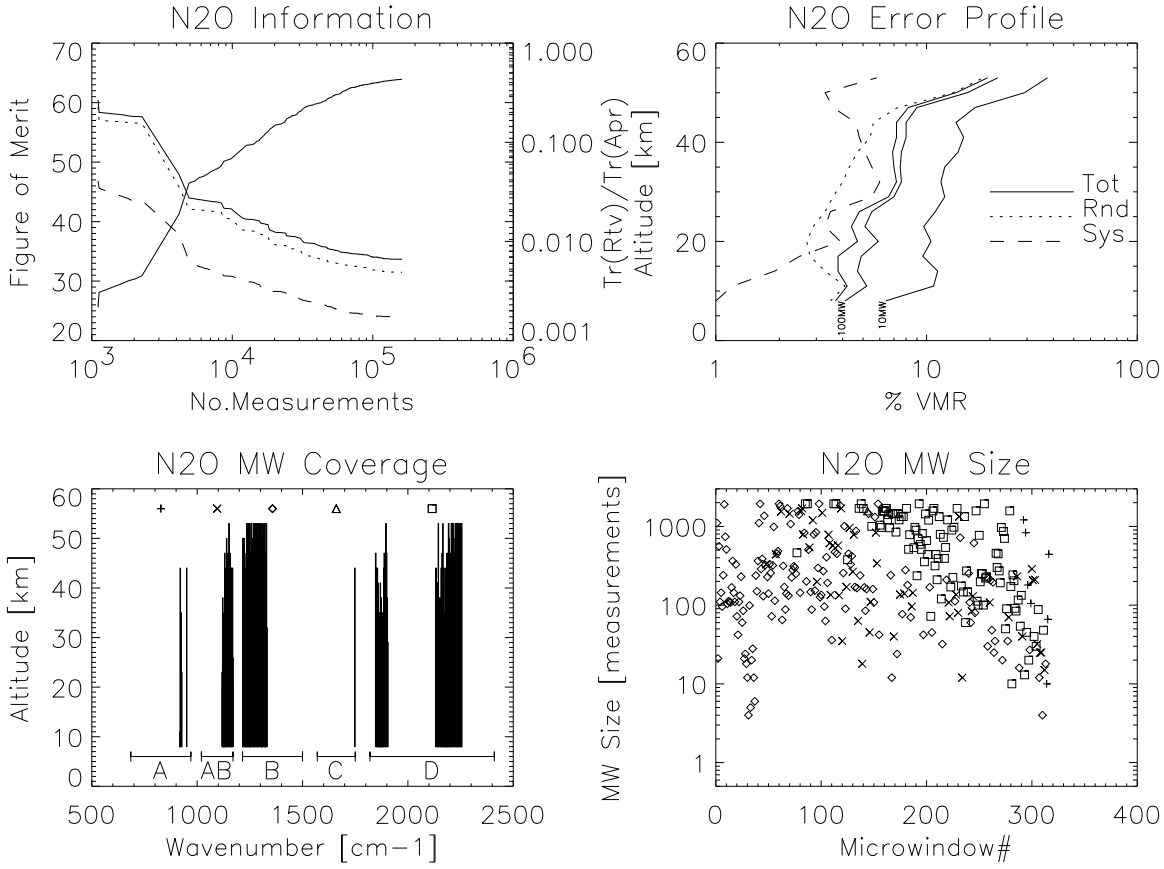

Figure 5: N_2O Results. Top left panel shows increase in information with number of measurements, along with reduction in trace of the error covariances (key as in top right). Top right shows final total error profile, together with profiles of the random and systematic error components. Also shown are the total error profiles after 10 and 100 microwindows have been selected. Bottom left plot shows wavenumber and altitude coverage of the microwindows. Bottom right plot shows band and size of microwindows as a function of selection number (see bottom left plot for key).

Table 5: N_2O Error contributions.

Microwindows = 582					Average size = 250 meas./MW					Used/Total meas. = 58995/145261 (41%)						
Alt	8km	11km	14km	17km	20km	23km	26km	29km	32km	35km	38km	41km	44km	47km	50km	53km
Rnd	3.4	4.2	4.1	4.0	3.9	3.1	3.2	3.6	3.0	3.6	4.5	5.4	5.3	5.3	9.2	12.2
Sys	2.5	1.5	2.1	2.9	3.4	5.0	7.8	10.1	16.3	16.3	15.7	13.8	11.9	8.6	6.9	6.1
Tot	4.2	4.5	4.6	4.9	5.2	5.9	8.4	10.8	16.5	16.7	16.3	14.9	13.0	10.1	11.5	13.7
Significant systematic error sources (largest error source at each altitude in bold).																
o3	0.1	0.1	0.2	0.4	0.9	1.1	2.5	2.5	1.8	0.9	0.6	0.2	0.7	0.4	0.4	0.0
ch4	0.4	0.4	1.0	1.4	1.5	1.5	2.9	2.5	2.8	2.3	1.7	1.0	0.7	0.1	0.5	0.2
hitran	**2.1**	**1.2**	**1.4**	1.5	1.6	1.1	2.0	1.0	1.9	2.2	1.9	1.1	2.7	1.5	1.2	1.6
gain	1.1	0.6	0.5	0.6	1.0	0.7	1.0	0.8	1.1	1.5	1.4	1.1	2.4	1.1	1.0	1.2
tem	0.2	0.4	1.0	**1.6**	**2.1**	**4.2**	**5.9**	**8.9**	**15.3**	**15.4**	**15.1**	**13.5**	**11.0**	**8.1**	**6.4**	**5.4**
los	0.3	0.4	0.4	0.5	1.0	1.5	2.0	2.4	3.7	3.5	2.7	2.2	2.1	2.1	1.9	1.6

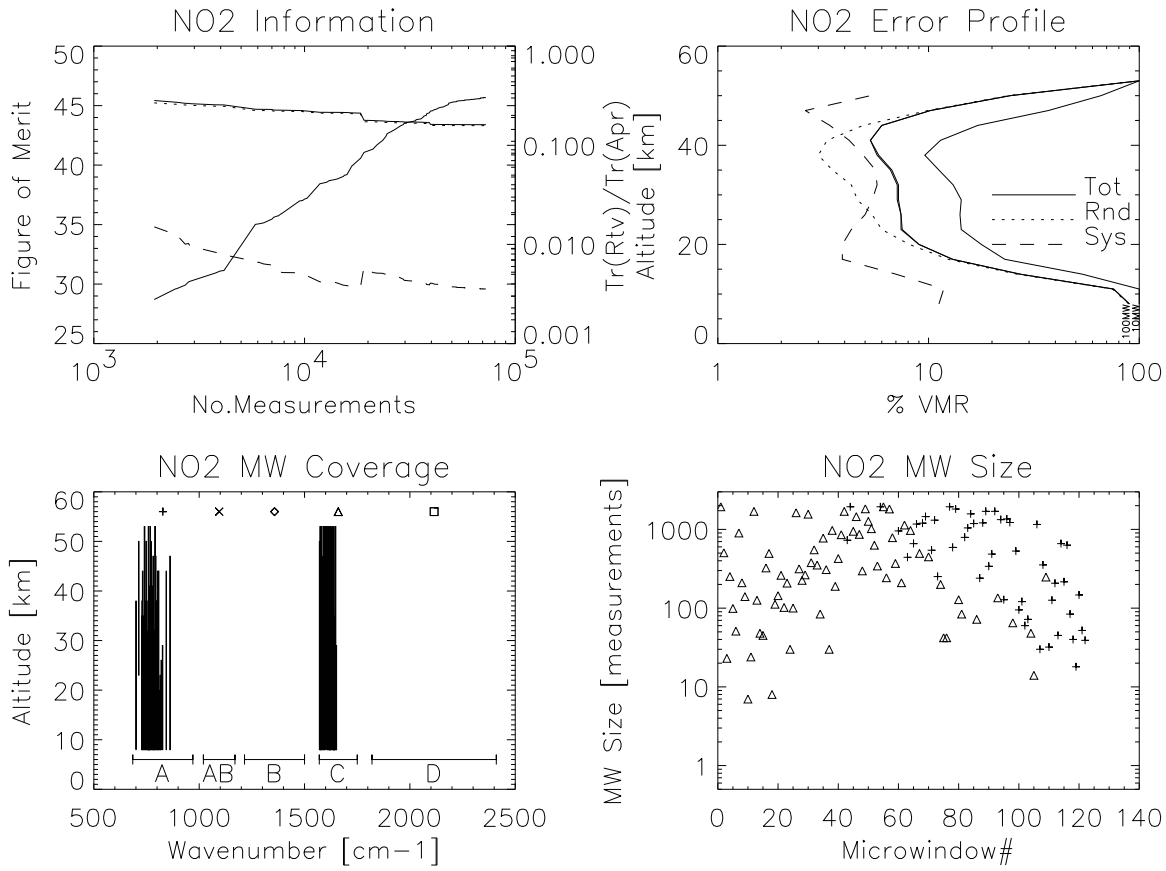

Figure 6: NO_2 Results. Top left panel shows increase in information with number of measurements, along with reduction in trace of the error covariances (key as in top right). Top right shows final total error profile, together with profiles of the random and systematic error components. Also shown are the total error profiles after 10 and 100 microwindows have been selected. Bottom left plot shows wavenumber and altitude coverage of the microwindows. Bottom right plot shows band and size of microwindows as a function of selection number (see bottom left plot for key).

Table 6: NO_2 Error contributions.

Microwindows = 365					Average size = 137 meas./MW					Used/Total meas. = 18250/49941(37%)						
Alt	8km	11km	14km	17km	20km	23km	26km	29km	32km	35km	38km	41km	44km	47km	50km	53km
Rnd	88.9	62.5	20.3	12.8	10.2	8.8	8.4	7.5	6.2	4.0	2.9	2.9	4.4	10.1	19.9	100
Sys	15.3	17.4	4.7	4.5	4.8	4.9	5.8	8.0	14.6	14.6	13.3	10.9	8.9	6.0	4.8	0.0
Tot	90.2	64.9	20.9	13.5	11.2	10.0	10.2	11.0	15.9	15.2	13.6	11.3	9.9	11.7	20.5	100
Significant systematic error sources (largest error source at each altitude in bold).																
h2o	**10.2**	7.2	1.0	0.0	0.8	1.1	1.5	2.0	2.6	0.6	1.0	0.8	1.0	1.2	1.0	0.0
ch4	0.1	0.9	0.1	0.6	1.4	1.2	1.1	0.8	0.0	0.1	0.2	0.0	0.3	0.2	0.0	0.0
hitran	3.2	5.9	**3.0**	2.7	2.7	2.2	2.4	2.5	1.6	1.1	1.1	1.8	1.3	0.8	2.5	0.0
gain	1.1	5.2	1.4	1.6	1.2	1.3	1.2	1.3	1.5	0.9	0.9	1.5	0.8	0.7	1.8	0.0
shift	7.9	5.1	0.1	0.5	0.0	0.1	0.4	0.0	0.4	0.4	0.3	0.4	0.0	0.3	0.9	0.0
tem	5.1	**9.3**	2.5	**2.8**	**3.0**	**3.4**	**4.2**	**7.0**	**13.9**	**14.3**	**13.0**	**10.4**	**8.5**	**5.4**	**3.2**	0.0
los	0.6	1.2	1.2	0.9	0.9	1.0	1.2	1.6	2.2	2.3	2.1	2.0	2.0	1.5	0.7	0.0

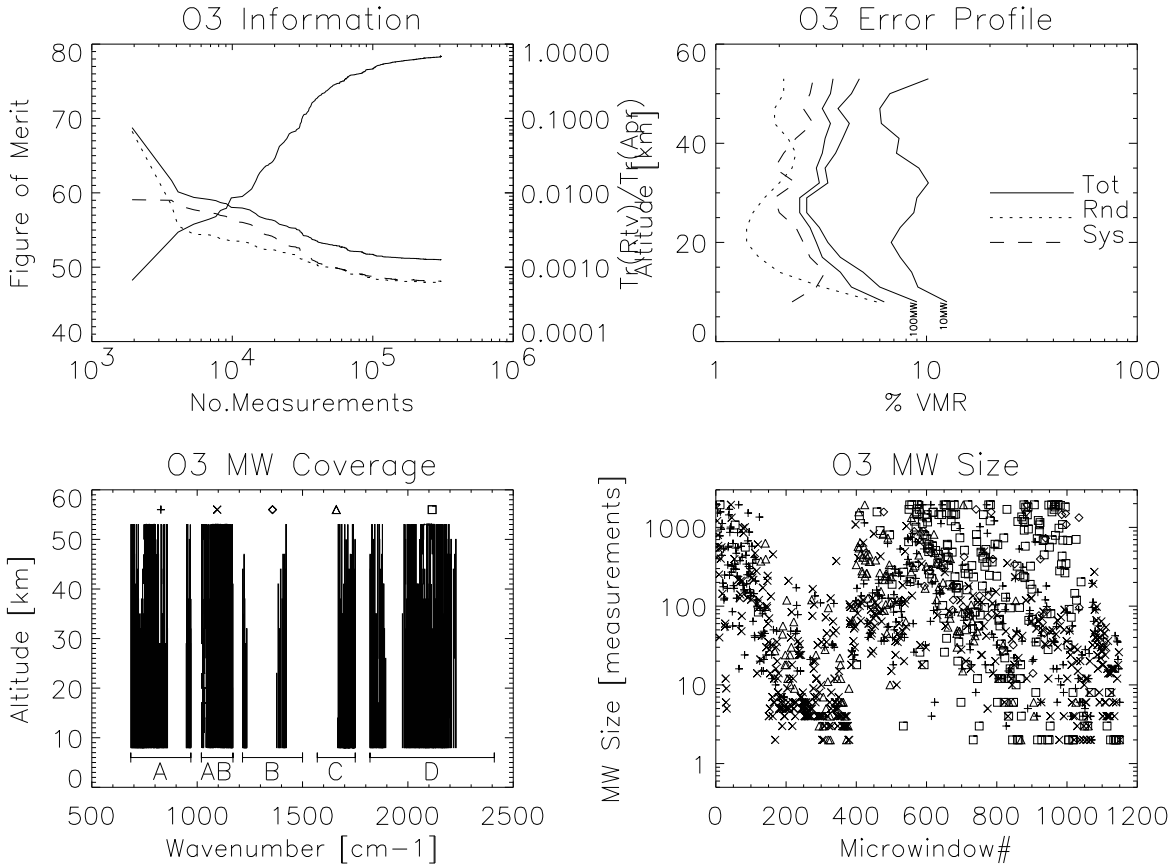

Figure 7: O_3 Results. Top left panel shows increase in information with number of measurements, along with reduction in trace of the error covariances (key as in top right). Top right shows final total error profile, together with profiles of the random and systematic error components. Also shown are the total error profiles after 10 and 100 microwindows have been selected. Bottom left plot shows wavenumber and altitude coverage of the microwindows. Bottom right plot shows band and size of microwindows as a function of selection number (see bottom left plot for key).

Table 7: O_3 Error contributions.

Microwindows = 1905					Average size = 101 meas./MW					Used/Total meas. = 73099/193207 (38%)						
Alt	8km	11km	14km	17km	20km	23km	26km	29km	32km	35km	38km	41km	44km	47km	50km	53km
Rnd	6.0	4.3	3.4	2.9	2.9	3.1	3.2	3.5	3.2	2.7	2.4	2.2	2.1	2.2	2.7	3.0
Sys	2.3	3.5	3.2	2.5	2.9	2.3	2.3	4.2	7.0	7.8	7.9	7.7	6.9	5.9	5.0	3.2
Tot	6.4	5.6	4.7	3.8	4.1	3.9	4.0	5.5	7.7	8.2	8.2	8.0	7.3	6.3	5.7	4.4
Significant systematic error sources (largest error source at each altitude in bold).																
hitran	**1.3**	**1.8**	**2.0**	**1.5**	**1.9**	**1.4**	**1.3**	1.8	1.9	1.7	1.7	1.2	0.9	0.8	0.8	0.7
gain	1.1	1.6	1.0	0.7	0.8	0.6	0.7	1.0	1.2	1.2	0.9	0.7	0.6	0.6	0.5	0.6
tem	1.2	1.6	1.3	1.1	1.3	0.9	1.3	**3.1**	**5.9**	**6.7**	**7.0**	**7.1**	**6.5**	**5.4**	**4.5**	**2.6**
los	0.8	**1.8**	1.6	1.3	1.4	1.2	**1.2**	1.7	2.8	3.2	2.9	2.4	2.1	2.0	2.0	1.5

a small plateau in the Figure of Merit plot before the curve starts to rise again.

HNO_3 Accuracies of 5–10% are obtainable up to 38 km, dropping off rapidly at higher altitudes. Temperature uncertainty is the dominant systematic error source at almost all altitudes, followed by HITRAN uncertainties, but total accuracy is limited by random errors below 14 km and above 35 km. Initially, most microwindows are selected from the B band but eventually the A and C bands. These microwindows often reach the maximum width (especially A band) but there is a decreasing trend in size with a large number of single-point microwindows at the end. Only 4 further microwindows were added when switching to F_0.

N_2O Retrieval accuracy of around 5% up to 26 km, 10–15% above that. Temperature uncertainty is the major error source from 23–47 km, random errors at higher and lower altitudes. HITRAN uncertainties contribute about 1–2% error at all altitudes, and are the largest systematic error source below 17 km. Microwindows are found in all bands, mainly B band to begin with then, as these decrease in size, mainly D band then A band. There is a single C band microwindow, (1746.8–1749.8 cm^{-1}) selected as #180. Only 4 microwindows were added when switching to F_0.

NO_2 Retrieval accuracy of 10–15% from 17–47 km, falling off rapidly above and below. The large random errors at high and low altitudes mean that the random and total covariance traces almost coincide. In the altitude range for useful retrievals, there is a clear divide at 29 km. Retrieval accuracy is limited by the temperature uncertainty above this, and by random errors below this. Microwindows are found in the C band initially, then in the A band, and gradually decrease in size. It should be remembered that this is based on a day-time NO_2 profile; at night-time, when NO_2 concentrations are significantly larger (especially above 40 km), better accuracy should be obtainable. Switching to F_0 from MW#221 onwards led to the selection of a large number of single point microwindows, all A-band and all at 8 km (apart from the very last microwindow). Since both NO_2 and microwindow-continuum are retrieved from this single measurement, the large (1000%) continuum *a priori* uncertainty seems to provide enough of a constraint for useful NO_2 information to be retrieved at that altitude when using the F_0 criterion, although not with the smaller emphasis on random error reduction using the F_3 criterion.

O_3 Retrieval accuracy of 5–10% for whole profile. Random errors around 3% from 14 km upwards, but dominant error up to 26 km. Above 29 km accuracy limited by temperature uncertainty. HITRAN uncertainty contributes 1–2% error at all altitudes, and is the dominant systematic error below 26 km. Microwindows are found in all bands, mostly small microwindows in the A and AB bands initially but eventually larger microwindows in the B, C and especially D bands. The switch from F_3 to F_0 occurs at MW#1708. Although this transition coincided with a modification to `MWMAKE` to suppress single-measurement microwindows, nevertheless a significant number of microwindows were added.

The temperature systematic error in the VMR retrievals shows the same general pattern of reaching a maximum around 30–35 km. The reduction at higher altitudes can be explained due to the increasing atmospheric temperature: a 3 K temperature uncertainty represents a smaller fraction of radiance at 270 K (50 km) than at 230 K (30 km), hence translates into a smaller error in retrieved concentration. At lower altitudes, although the atmospheric temperature reduces, the continuum retrieval presumably absorbs most of the temperature error: effectively the VMR is not fitted to the absolute value of the peak radiance, but depends more on the contrast between the peak and the continuum, and the size of this radiance difference reduces with altitude. This is supported by the observation that several of the VMR retrievals show a significant jump in the temperature-induced error at 32 km, the first altitude above the range over which the continuum profile is fitted (8–29 km).

6 Conclusions

The ultimate total error profiles are summarised in Fig. 8.

1. After the first one or two microwindows, accuracy increases fairly steadily as a function of the logarithm of the number of measurements (or microwindows) used, with only a gradual tailing off as the limit is approached. This makes it difficult to define an 'optimum' number of microwindows to use.

2. Temperature can apparently be retrieved to an absolute accuracy of 0.2–0.3 K at most altitudes, however this analysis does not take into account the effect of any horizontal gradients.

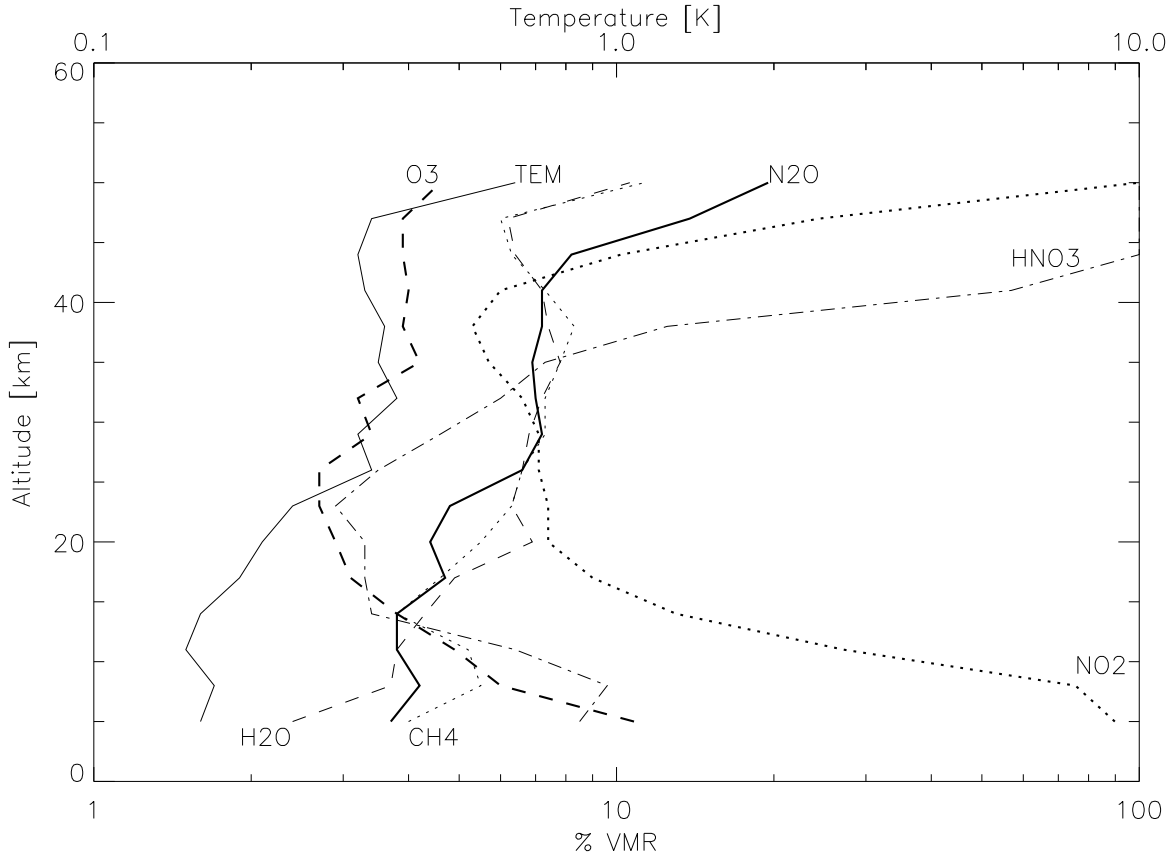

Figure 8: Summary of Ultimate Accuracy Results.

3. The assumed 3 K temperature uncertainty is the dominant term in the VMR retrievals (as expected, since radiance varies by several percent for a 1 K temperature increase). In a horizontally uniform atmosphere one could justify dividing this error by at least a factor 3 to obtain a truer estimate of ultimate accuracy (at mid-latitudes, at least).

4. When using a few tens of microwindows, the accuracy obtainable does not appear to be a strong function of the selection criterion (see Appendix).

5. Cross-contamination is not a significant limitation on the accuracy of the VMR retrievals, i.e., it is possible to select microwindows such that species can be retrieved without prior knowledge of other species concentrations. However, if other species concentrations are better known, the increased scope for microwindow selection will presumably still allow a reduction in other error terms.

6. Only independent retrievals have been considered here. Higher accuracy could be obtained by performing 'joint' retrievals (e.g., pT & H_2O, CH_4 & N_2O) and these probably represent a better use of extra cpu-processing time than adding more microwindows.

7. Given conclusions #2 and #3, it is probably better to model the effect of horizontal temperature gradients and temperature retrieval uncertainty separately rather than as a combined 3 K retrieval error. This would probably lead to improved VMR accuracy and worse temperature accuracy.

8. To reiterate two important caveats: this analysis applies only to mid-latitude, day-time conditions and no allowance has been made for the absolute uncertainty in HITRAN line strengths.

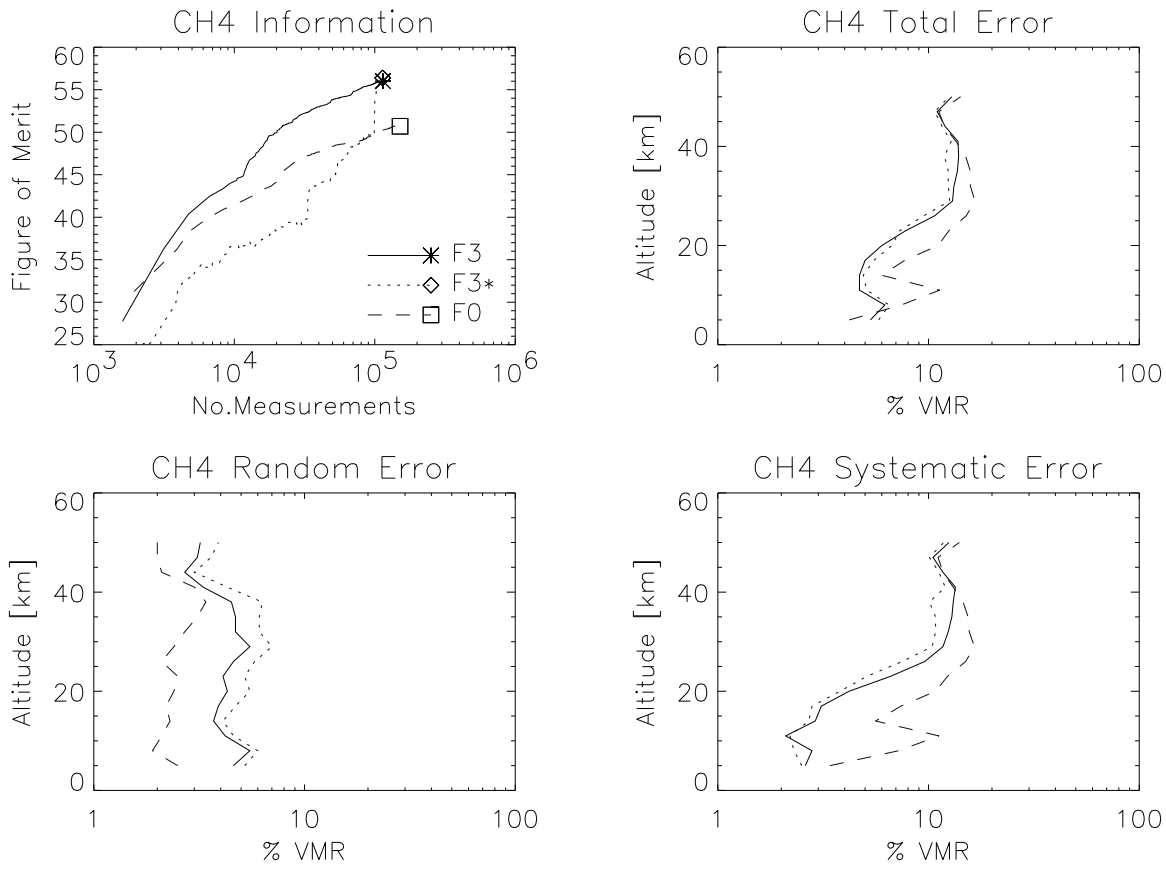

Figure 9: CH_4 Results for different selection criteria. See Appendix for details.

Appendix: Varying Selection Criteria

As mentioned in §4, the 3:1 sys:rnd weight should tend to bias the selection towards microwindows with larger random errors. The choice of weight is based on a crude assumption that the systematic error will remain constant while the random error reduces as $\sqrt{N}$ so, for about 20 microwindows, the two components will contribute equally to the total error. The trace plots in Figs. 1–7 actually show the systematic error also reducing as more microwindows are added, although not as rapidly as the random error contribution (HNO_3 and NO_2 being exceptions, where the trace is dominated by the high random errors outside the retrievable altitudes).

To examine the effect of this weighting, two further experiments have been performed, using just the CH_4 and NO_2 microwindows. Results are shown in Figs. 9 and 10, including the original F_3 selection for comparison.

1. Removing microwindows#1–20 from the set derived in §5, reusing all the remaining microwindows, then searching for new microwindows (including the possibility of using the spectral gaps left by the removal of #1–20) until no further improvement is found. This is shown as 'F3*' in the plots.

2. Constructing an entirely new set of microwindows based on the F_0 merit function, as described in §4, which simply minimises the total error.

In the first experiment it is assumed that, despite the 3:1 weighting, the first 20 microwindows will still contain a relatively large systematic error component compared to the subsequent microwindows. Therefore eliminating these microwindows should reduce the systematic error component of the total error, and allow scope for further microwindow selection that could exploit this and result in a higher final figure of merit compared to the original F_3 selection.

Results show that although the F_3* selection does indeed result in a selection with lower systematic errors, the selection process seems unable to exploit this and the final random error component is larger,

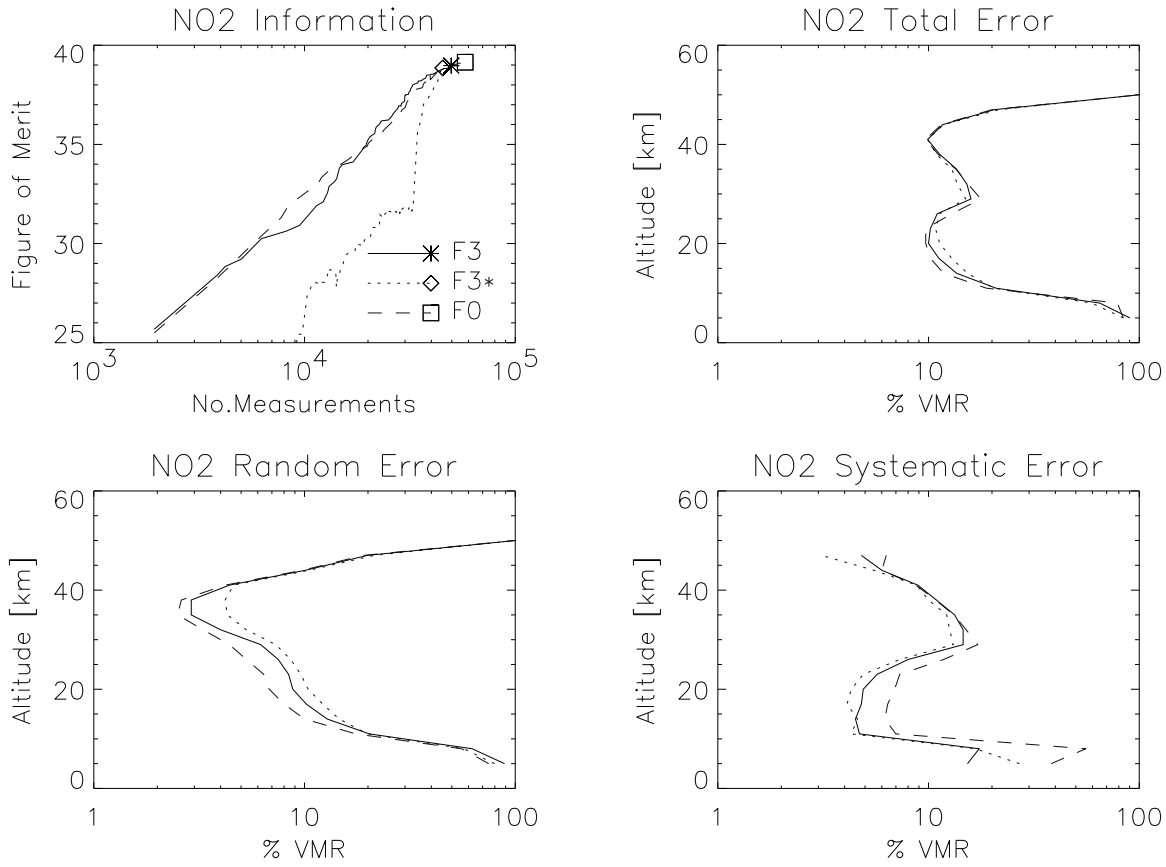

Figure 10: NO_2 Results for different selection criteria. See Appendix for details.

hence the figure of merit almost unchanged. A surprising feature is that the F_3* figure of merit curve (dotted line) increases roughly parallel to the original F_3 curve, and then converges rapidly once the new microwindows are added. This suggests that the information contained in the first 20 microwindows is fairly distinct and not simply reproduced by the remaining microwindows (in which case, the two curves would have converged gradually).

In the second experiment, no particular distinction is made between systematic and random errors so it is expected that the systematic error will grow more rapidly for this case, and that the final figure of merit will be reduced compared to the selection using F_3. It is also expected that the figure of merit will, initially, be larger for F_0 for a given number of measurements since the F_0 selection attempts to maximise the same figure of merit as used on the plots.

Results for CH_4 show the expected reduction in the final value of the F_0 figure of merit (dotted line) compared to F_3, and that the F_0 value is initially, although briefly, higher. For NO_2 there is very little difference between the curves, both during the selection and at the final value reached. However, for both gases, the final random and systematic error profiles for F_0 are smaller and larger, respectively, than for the F_3 selection, as expected.

From these limited tests it is concluded that biasing the initial selection towards low systematic errors is probably beneficial when hundreds of microwindows are used, but less obviously so when using only tens of microwindows.

References

[1] Echle, G. *et al*, Optimised Spectral Microwindows for MIPAS-Envisat Data Analysis. Submitted to *App. Optics*, 2000.

[2] Dudhia, A. A Multilayer technique for microwindow selection. *Tech. Note presented at MIPAS SAG-30*, April 1998.

[3] Bennett, V., A. Dudhia and C. D. Rodgers. Microwindow selection for MIPAS using information content. *Proceedings of ESAMS '99*, ESTEC, January 1999.

[4] Nett, H., MIPAS NESR_T data. From first TV performance test campaign (before vibration test). March 1999.

[5] Remedios, J. J., Extreme Atmospheres for MIPAS, v2.1. *CCN4 of contract PO-MA-OXF-GS-0003*, June 1999.

[6] Clarmann, T.v., *et al*, Study on the Simulation of Atmospheric Infrared Spectra, *Final Report, ESA Contract 12054/96/NL/CN*, August 1998.